Stability analysis for linear discretisations of the advection equation with Runge–Kutta time integration

Michael Baldauf *

Abteilung Meteorologische Analyse und Modellierung, Deutscher Wetterdienst, Kaiserleistrasse 42, D-63067 Offenbach, Germany

Abstract

For the 1-dim. linear advection problem stability limits of Runge–Kutta (RK) methods from 1st to 7th order in combination with upwind or centered difference schemes from 1st to 6th order are presented. The analysis can be carried out in a rather general way by introduction of a broad class of Runge–Kutta methods, here called 'Linear Case Runge–Kutta (LC-RK)' methods, which behave completely similar for linear, time-independent and homogeneous ODE-systems and contain the 'classical' order = stage RK methods. The set of conditions for the coefficients of these LC-RK-schemes could be derived explicitly for arbitrary order N. From an efficiency viewpoint the LC-RK 3rd order methods in combination with upwind 3rd or 5th order or the LC-RK 4th order scheme with 4th order centered difference advection are a good choice. The analysis can be extended easily to multidimensional splited advection for which a necessary stability condition is presented.
© 2008 Elsevier Inc. All rights reserved.

1. Introduction

The dynamic equations of meteorology build up a rather stiff system of PDE's. Sound expansion, especially in vertical direction, takes place on much shorter time scales than horizontal advection or even Coriolis accelerations. For discretising the fast processes sometimes implicit methods are used; often in form of a semi-implicit semi-Lagrangian scheme, as it is used e.g. in the Unified Model of the British Weather Service [1]. Another method discretises only the vertical direction implicitly and the horizontal directions explicitly. The result of this procedure is an only weakly stiff PDE-system. To efficiently solve this, a time splitting (sometimes called 'partial operator splitting' or 'subcycling') is carried out where a distinction is made between small and large timesteps. With that the fast processes (sound expansion and buoyancy, leading to the expansion of gravity waves) and slow processes (especially the horizontal advection) can be integrated. In [2] this fundamental idea of time splitting was proposed and realized with a 3-timelevel leapfrog scheme.

* Tel.: +49 69 8062 2733; fax: +49 69 8062 3721.
  E-mail address: michael.baldauf@dwd.de

As in most computational fluid dynamic (CFD)-applications and in meteorological modelling, the exact description of the advection process is of fundamental importance for a successful simulation. Due to the wide variety of internal structures arising in the atmosphere, the usual approach is to use a relatively large number of grid points (currently about 10^7–10^8 in weather forecast models) and to use very fast algorithms, e.g. a 24-hour forecast (globally as well as for the European area) has to be calculated in less than half an hour on an 'ordinary' supercomputer at the German Weather Service (DWD). Therefore relatively simple but fast spatial discretisations for the advection terms are often used. Besides in meteorology shock-capturing is not of major concern. This is to some extent contrary to many other CFD fields, where a nonlinear stability property like total variation diminishing (TVD) or bounded in time (TVB) is required, perhaps additionally to linear stability properties (e.g. [3]). This lent to the inspection of sub-classes of Runge–Kutta (RK) methods like the TVD-RK method [4] or more generally the strong-stability preserving RK methods [5].

Especially the WRF-model (e.g. [6,7]), used for scientific purposes as well as for weather forecasting in the USA, combines upwind advection schemes with a Runge–Kutta (RK) time integrator. This is now also applied in the COSMO-model system for the 'dynamical' variables velocity u, v, w, temperature perturbation T', and pressure perturbation p'. The COSMO-model is currently applied at several European weather forecast centers, e.g. at the German weather service (DWD) as COSMO-DE model (formerly known as LMK model) or at MeteoSwiss as COSMO-S2 and COSMO-S7. It should be remarked here that for the moisture variables and the turbulent kinetic energy, flux corrected finite volume methods [8] or Semi-Lagrangian-schemes of a high interpolation order (see [9] for an overview) are used outside of the time splitting scheme.

One goal in this partial operator splitting viewpoint is the search for advection schemes which allow large timesteps. In [7] stability limits in the case of 2nd and 3rd order RK methods and for several upwind and centered difference advection schemes were given. The Courant number limits suggest, that an increase of the order of a RK method would also allow larger timesteps. This is not generally the case, which is demonstrated in the following, at least for the spatial discretisations presented here.

The aim of this work is the systematic calculation of stability limits for Runge–Kutta methods up to 7th order in combination with upwind or centered difference schemes up to 6th order. In a relatively broad number of cases even an analytical expression for the limiting Courant number can be presented. We want to remark, that for these schemes the important theorem of Shu [4,3,5] about the CFL-condition for strong stability cannot be applied, because (with the exception of the upwind scheme of first order, the donor cell method) all spatial discretisations are unstable with an Euler-forward step (see below).

In Section 2 it is shown, that it is not necessary to make a distinction between different Runge–Kutta methods of a certain order. One can even define a very large class of RK-methods with exactly the same linear stability properties; those are called here 'Linear Case-RK (LC-RK) methods'. One example for such a 3rd order LC-RK method is used in [7] for the WRF model. This class contains the 'classical order = stage for nonlinear equations' RK-methods. This distinguishes this paper also from other works which inspect RK-methods of lower order than stage. For computational aeroacoustic applications schemes with only small dispersion and dissipation errors were constructed by a minimization of the integral error of the effective wavenumber ([10,11]). Such an optimization can even lead to schemes which depend explicitly from the initial conditions [12]. In Section 3 the stability limits for LC-RK methods for different linear, spatial discretisations of the one-dimensional advection operator are calculated. To show the relevance of the stability statements some numerical experiments are carried out in Section 4. Section 5 will present an extension to the space splitted multi-dimensional case. Section 6 makes an assessment about the efficiency of these schemes.

2. A linear view to explicit Runge–Kutta-schemes

For a system of M ordinary differential equations (ODE's)

$$\frac{\mathrm{d}q_l}{\mathrm{d}t} = f_l(t, q_1, \ldots, q_M), \quad l = 1, 2, \ldots, M, \tag{1}$$

the general explicit N-stage Runge–Kutta method to advance the solution from timestep t^n to $t^{n+1} = t^n + \Delta t$ reads

$$q_l^{(0)} := q_l^n,$$
$$k_l^{(i)} := f_l(t^n + \Delta t \cdot \alpha_i, \mathbf{q}^{(i-1)}),$$
$$q_l^{(i)} := q_l^n + \Delta t \cdot \sum_{j=1}^{i} \beta_{i+1,j} k_l^{(j)}, \tag{2}$$
$$q_l^{n+1} := q_l^{(N)},$$

$l = 1, 2, \ldots, M$, $i = 1, 2, \ldots, N$. We abbreviated $q_i^n = q_i(t^n)$ and denote by $\mathbf{q} = (q_1, q_2, \ldots, q_M)$ the vector of all variables of the ODE-system. The coefficients are often written in the so called Butcher–Tableau [13]:

$$
\begin{array}{c|ccccc}
0 & & & & & \\
\alpha_2 & \beta_{21} & & & & \\
\alpha_3 & \beta_{31} & \beta_{32} & & & \\
\ldots & \ldots & \ldots & & & \\
\alpha_N & \beta_{N1} & \beta_{N2} & \ldots & \beta_{N,N-1} & \\
\hline
& \beta_{N+1,1} & \beta_{N+1,2} & \ldots & \beta_{N+1,N-1} & \beta_{N+1,N}
\end{array}
$$

There exist several different forms of writing the RK schemes. One of the most general form is used in [5,3]. In older texts there are often introduced new coefficients $b_j \equiv \beta_{N+1,j}$ (e.g. [13,14]); but without them the most following formulas can be written more compact (this is also remarked in [13, p. 163]).

To arrive at a certain convergence order, the coefficients must fulfill some constraints. These can be derived in the following manner; done here only for one variable. In the following we limit ourselves to autonomous ODE-systems, analogous to [13], which simplifies the constraints to a certain extent. At first, the total derivatives of q are expressed with the aid of the original ODE-system by the right hand side f and its derivatives

$$\frac{\mathrm{d}q}{\mathrm{d}t} = f(q), \tag{3}$$

$$\frac{\mathrm{d}^2 q}{\mathrm{d}t^2} = \frac{\mathrm{d}}{\mathrm{d}t}\frac{\mathrm{d}q}{\mathrm{d}t} = \frac{\mathrm{d}f}{\mathrm{d}q}\frac{\mathrm{d}q}{\mathrm{d}t} = f_{,q}f, \tag{4}$$

$$\frac{\mathrm{d}^3 q}{\mathrm{d}t^3} = \frac{\mathrm{d}}{\mathrm{d}t}\frac{\mathrm{d}^2 q}{\mathrm{d}t^2} = f_{,q,q}f^2 + f_{,q}^2 f, \tag{5}$$

$$\frac{\mathrm{d}^4 q}{\mathrm{d}t^4} = \frac{\mathrm{d}}{\mathrm{d}t}\frac{\mathrm{d}^3 q}{\mathrm{d}t^3} = f_{,q,q,q}f^3 + 4f_{,q,q}f_{,q}f^2 + f_{,q}^3 f, \tag{6}$$

$$\ldots$$

These are put into the Taylor expansion of the function

$$q(t + \Delta t) = q(t) + \Delta t \frac{\mathrm{d}q}{\mathrm{d}t} + \frac{1}{2}\Delta t^2 \frac{\mathrm{d}^2 q}{\mathrm{d}t^2} + \frac{1}{3!}\Delta t^3 \frac{\mathrm{d}^3 q}{\mathrm{d}t^3} + \cdots, \tag{7}$$

which can now be compared order by order with the Taylor expansion by Δt of the general RK method (2). The constraints are found by comparing the different orders Δt^i and for a certain order i by comparison of the coefficients of f, $f_{,q}f$, ... Dependent from how far this procedure is carried out, one obtains an N-stage RK method of order N'. These calculations become very tedious with increasing order; [13] uses a special graph theory for their economic calculation and can show for example that for nonlinear ODE-systems the maximum reachable order N' can be less than the stage N of the RK method. [14] derives these conditions with a 'linear representation' of the RK-equations and a subsequent recursion to circumvent the graph theoretical approach. At least the so called consistency condition

$$\sum_{i=1}^{N} \beta_{N+1,i} = 1 \tag{8}$$

has to be fulfilled. It is both necessary and sufficient to get a local truncation error of $O(\Delta t^2)$ [13, p. 131,15]. Strictly speaking, for autonomous ODE's the coefficients α_i are not needed. In this case [13] defined them by

$$\alpha_i := \sum_{j=1}^{i-1} \beta_{ij}, \tag{9}$$

which are indeed the $N-1$ conditions needed for non-autonomous systems.

According to the further constraints one can show that there exist exactly one explicit first order Runge–Kutta method (the Euler forward scheme), a 1-parametric family of explicit 2nd stage, 2nd order RK methods, a 2-parametric family of explicit 3rd stage, 3rd order RK methods, an also 2-parametric family of explicit 4th stage, 4th order RK methods, and so on (e.g. [16]). The general conditions in the nonlinear case up to 4th order are listed in the Appendix A.

2.1. 'Linear Case Runge–Kutta' methods for linear operators

Now we consider a linear, homogeneous and time-independent ODE-system of the form

$$\frac{\mathrm{d}q_l}{\mathrm{d}t} = f_l(q_1, \ldots, q_M) = \sum_{j=1}^{M} P_{lj}\, q_j, \quad l = 1, 2, \ldots, M, \tag{10}$$

or in vector notation

$$\frac{\mathrm{d}\mathbf{q}}{\mathrm{d}t} = \mathbf{P}\mathbf{q}. \tag{11}$$

The time-independence implies that the P_{ij} are constant coefficients. In the case of only one equation $M=1$ this is called the 'standard-testproblem' [13] or the 'Dahlquist test equation' [17,18]. We note that in particular linear PDE's and PDE-systems can be described, which are semi-discretized by the 'method of lines', e.g. equations of the form (74).

Lemma 2.1. *For the linear, homogeneous ODE-system* (10) *with a constant coefficient matrix* $\mathbf{P}$ *the N-stage Runge–Kutta method* (2) *($N = 0, 1, 2, 3, \ldots$) is of the form*

$$\mathbf{q}^{(N)} = (1 + \Delta t\mathbf{P}h_{N+1}^{(1)} + \Delta t^2\mathbf{P}^2 h_{N+1}^{(2)} + \cdots + \Delta t^N \mathbf{P}^N h_{N+1}^{(N)})\mathbf{q}^{(0)} = \left(\sum_{k=0}^{N} (\Delta t\mathbf{P})^k h_{N+1}^{(k)}\right)\mathbf{q}^{(0)}, \tag{12}$$

with the following recursively defined abbreviations:

$$h_i^{(0)} := 1, \quad i = 1, 2, 3, \ldots, \tag{13}$$

$$h_i^{(1)} := \sum_{j=1}^{i-1} \beta_{ij} h_j^{(0)} = \sum_{j=1}^{i-1} \beta_{ij}, \quad i = 2, 3, \ldots, \tag{14}$$

$$\cdots$$

$$h_i^{(l)} := \sum_{j=l}^{i-1} \beta_{ij} h_j^{(l-1)}, \quad i = l+1, l+2, \ldots, \tag{15}$$

$$\cdots$$

The bracketed term in (12) is often called the stability function R: $\mathbf{q}^{(N)} = R(\Delta t\mathbf{P})\mathbf{q}^{(0)}$ [18]. We want to mention, that the $h_i^{(1)}$ are identical with the coefficients α_i from Eq. (9) occuring in the Butcher Tableau. This result is already sketched in [17, p. 16], but without the correct summation indices. Therefore we will give a proof done by complete induction. The lemma is trivially fulfilled for $N = 0$. For the conclusion from $0, 1, 2, \ldots, N$ to $N+1$ we start from definition (2) of the RK method applied to (10)

$$\mathbf{q}^{(N+1)} = \mathbf{q}^{(0)} + \Delta t \sum_{j=1}^{N+1} \beta_{N+2,j} \mathbf{P}\mathbf{q}^{(j-1)}. \tag{16}$$

Now we use the induction hypothesis

$$\mathbf{q}^{(N+1)} = \mathbf{q}^{(0)} + \Delta t \sum_{j=1}^{N+1} \beta_{N+2,j} \mathbf{P} \left(\sum_{l=0}^{j-1} (\Delta t \mathbf{P})^l h_j^{(l)} \right) \mathbf{q}^{(0)}. \tag{17}$$

The sequence of the summation can be exchanged to

$$\mathbf{q}^{(N+1)} = \left(1 + \sum_{l=0}^{N} (\Delta t \mathbf{P})^{l+1} \sum_{j=l+1}^{N+1} \beta_{N+2,j} h_j^{(l)} \right) \mathbf{q}^{(0)} \tag{18}$$

and with a renaming of the summation $l + 1 = l'$ we get

$$\mathbf{q}^{(N+1)} = \left(\sum_{l'=0}^{N+1} (\Delta t \mathbf{P})^{l'} \underbrace{\sum_{j=l'}^{N+1} \beta_{N+2,j} h_j^{l'-1}}_{(*)} \right) \mathbf{q}^{(0)}. \tag{19}$$

Term $(*)$ is exactly the definition of $h_{N+2}^{(l')}$ which finishes the conclusion to $N + 1$.

An explicit expression for the coefficients is

$$h_i^{(l)} = \sum_{j_l=l}^{i-1} \sum_{j_{l-1}=l-1}^{j_l-1} \cdots \sum_{j_2=2}^{j_3-1} \sum_{j_1=1}^{j_2-1} \beta_{ij_l} \cdot \beta_{j_l j_{l-1}} \cdots \beta_{j_3 j_2} \cdot \beta_{j_2 j_1}, \quad i = l+1, l+2, \dots$$

This can be derived directly from Eq. (15) or can again easily be proved by induction.

Theorem 2.1. *For the linear, homogeneous ODE-system* (11) *with a constant coefficient matrix* $\mathbf{P}$ *the N-stage Runge–Kutta method* $(N = 0, 1, 2, 3, \dots)$ *has the form* (12) *and is of order* N', *if the following conditions are fulfilled*:

$$h_{N+1}^{(l)} = \frac{1}{l!}, \quad l = 1, 2, \dots, N', \ N' \leqslant N. \tag{20}$$

Proof (*see also* [17]). Due to the time-independency of the $\mathbf{P}_{ij}$ the formal solution of (10) is

$$\mathbf{q}^{n+1} = e^{\Delta t \mathbf{P}} \mathbf{q}^n. \tag{21}$$

The formulation (12) from Lemma 2.1 with the N' conditions (20) is exactly its expansion up to order N'. $\quad\square$

To sum it up, Lemma 2.1 makes a statement about the form of all RK-schemes applied to the linear ODE-system whereas Theorem 2.1 determines their order.

In the special case $N' = N$ we will call such a RK method a Linear Case Runge–Kutta method of stage N or of order N (LC-RK method of order N). We want to emphasize here, that for these LC-RK methods, Eq. (12) with conditions (20) is indeed an exact result and not only the first terms of a Taylor expansion. Therefore, for the following section the important conclusion is: all different LC-RK methods of a certain order N behave exactly identical for the linear, homogeneous ODE-system (10); in particular they possess the same stability properties for such ODE-systems. The particular conditions up to order 4 are listed in Appendix A.

A simple solution of these conditions for an LC-RK method of order N is

$$\beta_{i+1,i} = \frac{1}{N-i+1}, \quad i = 1, 2, \dots, N, \qquad \beta_{ij} = 0 \quad \text{otherwise.} \tag{22}$$

This can be easily proved: insertion of these $\beta_{i,j}$ in the definition of the $h_i^{(l)}$ (13)–(15) gives

$$h_i^{(l)} = \frac{1}{N-i+2} h_{i-1}^{(l-1)}, \quad i = l+1, l+2, \dots, N+1, \ l = 1, 2, \dots \tag{23}$$

Starting from $l = 1$ one can show successively that the conditions (20) can be fulfilled.

For $N = 3$ this is just the scheme proposed in [7] for the WRF-model; or e.g. for an LC-RK of order 5:

$$
\begin{array}{c|ccccc}
0 & & & & & \\
\alpha_2 & 1/5 & & & & \\
\alpha_3 & 0 & 1/4 & & & \\
\alpha_4 & 0 & 0 & 1/3 & & \\
\alpha_5 & 0 & 0 & 0 & 1/2 & \\
\hline
& 0 & 0 & 0 & 0 & 1
\end{array}
$$

Lemma 2.2. *Those Runge–Kutta methods, whose order N is equal to their stage N also for nonlinear problems, are a subset of the Linear Case RK methods of order N.*

Proof. For the linear, homogeneous ODE-system (10) one can deduce by successive derivation

$$
\frac{d^k \mathbf{q}}{dt^k} = \mathbf{P}^k \mathbf{q} = \left(\frac{\partial \mathbf{f}}{\partial \mathbf{q}} \right)^{k-1} \mathbf{f}, \tag{24}
$$

because the Jacobian matrix is just $\partial \mathbf{f} / \partial \mathbf{q} = \mathbf{P}$. Obviously these are the most rightstanding terms on the r.h.s. of the general higher derivatives of q in (3), (4),…Therefore in the linear case we have to fulfill only a subset of the conditions valid for the general nonlinear case. $\square$

In particular all 'order = stage' RK methods of a certain order behave identically to the linear, homogeneous ODE-system (10). Therefore the 2nd, 3rd and 4th order RK-schemes mentioned in [19] or the 3rd order TVD-RK scheme in [20], which is described as the optimal 3rd stage, 3rd order SSP(3,3)-RK method in [5], are also examples of LC-RK schemes.

However, a time splitting of the type [6] is not covered by this analysis. There, a different ratio occurs between the fast and slow operators in every RK substep, and therefore a time-dependency of the P's exists indirectly.

Simply speaking, an LC-RK Nth order scheme is of Nth order for linear problems, but in general of less order for nonlinear or time-dependent problems. The reason to consider them is that they behave similarly to linear, homogeneous ODE-systems. Moreover to derive linear stability constraints more or less analytically or even only by numerical experimentation it is sufficient to consider (or program) only the most simple version e.g. (22). It should be mentioned that the development of the strong stability preserving RK-methods follow a different guideline: their order N' is generally lower than their stage N, even in the linear case, e.g. the SSP(4,3) scheme in [5] fulfills only the first three conditions (A.8), (A.9), and (A.11) of a LC-RK 4th order method, but not the 4th condition (A.15).

3. Linear one-dimensional advection

Our aim is the stability analysis of the linear advection equation with constant velocity u

$$
\frac{\partial q}{\partial t} = \mathcal{F} q = -u \frac{\partial q}{\partial x} = -\frac{\partial u q}{\partial x}. \tag{25}
$$

After a spatial discretisation, e.g. with the 'method of lines' (as usual $q_j(t) \equiv q(x_j, t)$), the following ODE-system can be solved numerically with an ODE-solver like a Runge–Kutta method. If the discretisation scheme and the boundary conditions are linear, too, then the resulting ODE-system has the form (10). [7,19] present spatial discretizations of the flux form with the advection flux

$$
F(q) = u q. \tag{26}
$$

In the case considered here advection-form and flux-form and also their upwind or centered difference discretisations are identical; in the following we will consider only the advection form of the operator $\mathcal{F}$:

'up1' : $\qquad f_j^{(1)}(q) := -u \dfrac{q_j - q_{j-1}}{\Delta x},$ $\hfill (27)$

'cd2' : $\qquad f_j^{(2)}(q) := -u \dfrac{q_{j+1} - q_{j-1}}{2\Delta x},$ $\hfill (28)$

'up3' : $\qquad f_j^{(3)}(q) := -u \dfrac{2q_{j+1} + 3q_j - 6q_{j-1} + q_{j-2}}{6\Delta x},$ $\hfill (29)$

'cd4' : $\qquad f_j^{(4)}(q) := -u \dfrac{-(q_{j+2} - q_{j-2}) + 8(q_{j+1} - q_{j-1})}{12\Delta x},$ $\hfill (30)$

'up5' : $\qquad f_j^{(5)}(q) := -u \dfrac{-3q_{j+2} + 30q_{j+1} + 20q_j - 60q_{j-1} + 15q_{j-2} - 2q_{j-3}}{60\Delta x},$ $\hfill (31)$

'cd6' : $\qquad f_j^{(6)}(q) := -u \dfrac{(q_{j+3} - q_{j-3}) - 9(q_{j+2} - q_{j-2}) + 45(q_{j+1} - q_{j-1})}{60\Delta x}.$ $\hfill (32)$

These formulae are simply the derivative $\partial q / \partial x$ up to the appropriate order with the least width of the stencil, so called optimal-order schemes. In the following we will use the abbreviations up1, up3, up5 and cd2, cd4, cd6 for these upwind and centered difference discretisations of the appropriate order.

We carry out a von-Neumann stability analysis similar e.g. to the methodology in [18, p. 111] (see also the remarks in Section 4). The Fourier transformation

$$q_j(t) = \sum_k \tilde{q}_k(t) e^{ikj\Delta x} \hfill (33)$$

converts the semi-discrete system to an appropriate system for $\tilde{q}_k(t)$, which again possess the form (10). Assuming periodic boundary conditions its matrix **P** is even diagonal and as usual for von-Neumann-analysis it is sufficient to consider only single wave lengths. This generates the decoupled equations

$$\frac{d\tilde{q}_k}{dt} = -i \frac{1}{\Delta t} C d(k) \tilde{q}_k, \hfill (34)$$

where the factor $d(k)$ is a polynomial in $e^{\pm ik\Delta x}$ (with constant coefficients) and is solely determined by the spatial discretisation. C is the Courant number $C := u\Delta t / \Delta x$ and the factor Δt was extracted so that $d(k)$ becomes dimensionless. d is sometimes called *effective (dimensionless) wavenumber* (e.g [10]), because it is identical with $k\Delta x$ in the continuous case (that is the reason why the factor $-iC$ was extracted, too).

For the numerical operators (27)–(32) we get with the dimensionless wave number $K := k\Delta x$ the following effective wavenumbers:

$$d_{(1)} = i(e^{-iK} - 1), \hfill (35)$$

$$d_{(2)} = \sin K, \hfill (36)$$

$$d_{(3)} = -i \frac{2e^{iK} + 3 - 6e^{-iK} + e^{-i2K}}{6}, \hfill (37)$$

$$d_{(4)} = -\frac{1}{6} \sin 2K + \frac{4}{3} \sin K, \hfill (38)$$

$$d_{(5)} = i \frac{3e^{2iK} - 30e^{iK} - 20 + 60e^{-iK} - 15e^{-i2K} + 2e^{-i3K}}{60}, \hfill (39)$$

$$d_{(6)} = \frac{1}{30} \sin 3K - \frac{9}{30} \sin 2K + \frac{45}{30} \sin K. \hfill (40)$$

Discretising Eq. (34) with an LC-RK method of order N one gets

$$\tilde{q}_k^{n+1} = A(k) \tilde{q}_k^n, \hfill (41)$$

where due to Theorem 2.1 the amplification-factor $A(k)$ has the form

$$A(k) = 1 + z + \frac{z^2}{2!} + \cdots + \frac{z^N}{N!}, \quad z = -iCd(K). \hfill (42)$$

From this follows the close relationship between linear stability and approximation order of the Runge–Kutta methods.

3.1. Results of the stability analysis

We now want to calculate stability limits. In [18, Section II.1.4] the critical Courant numbers for RK from 1st to 4th order in combination with up1, cd2, up3, and cd4 spatial discretization were calculated. There it was done by numerically estimating the maximum of the amplification factor $|A|$. The question now is the following: can RK methods of even higher order result in a higher stability range and therefore in higher efficiency? Therefore RK5, RK6, and RK7 are considered also with higher spatial discretizaions up5 and cd6. In [7] the stability limits for RK2 and RK3 and discretizations from up3 to cd6 were calculated (assumedly) by numerical experimentation. [10] searched RK-schemes for centered difference spatial discretisations of the advection operator which are largely stable and also have a high degree of accuracy. The RK-schemes they found are not a subclass of the LC-RK schemes, but it is interesting, that their optimization procedure delivered coefficients $h_{N+1}^{(l)}$ of the stability function that are rather close to $1/l!$ of the LC-RK-schemes (see their Table 2). Their approach was improved by [11] who found optimized RK-schemes which allow higher Courant numbers in connection with optimized centered difference schemes.

In the following partly analytical results for the critical Courant number can be achieved.

3.1.1. Consideration of centered difference schemes

The square modulus of the amplification-factor $|A(k)|^2$ obviously can be written as a real polynomial in the real and imaginary parts of $z = r + is$, therefore $r = \text{Im}(Cd(K))$ and $s = -\text{Re}(Cd(K))$. The stability analysis of centered difference schemes is in a certain way more lucid than that of upwind schemes, because in c.d.-schemes $d(k)$ is purely real and z is purely imaginary, i.e. $r = 0$. For the case of a discretisation with centered differences $|A(k)|^2$ simplifies to

$$\text{LC-RK 1st order}: \quad |A(k)|^2 = 1 + s^2, \tag{43}$$

$$\text{LC-RK 2nd order}: \quad |A(k)|^2 = 1 + \frac{s^4}{4}, \tag{44}$$

$$\text{LC-RK 3rd order}: \quad |A(k)|^2 = 1 - \frac{s^4}{(3!)^2}(3 - s^2), \tag{45}$$

$$\text{LC-RK 4th order}: \quad |A(k)|^2 = 1 - \frac{s^6}{(4!)^2}(8 - s^2), \tag{46}$$

$$\text{LC-RK 5th order}: \quad |A(k)|^2 = 1 + \frac{s^6}{(5!)^2}(40 - 15s^2 + s^4), \tag{47}$$

$$\text{LC-RK 6th order}: \quad |A(k)|^2 = 1 + \frac{s^8}{(6!)^2}(180 - 24s^2 + s^4), \tag{48}$$

$$\text{LC-RK 7th order}: \quad |A(k)|^2 = 1 - \frac{s^8}{(7!)^2}(1260 - 504s^2 + 35s^4 - s^6). \tag{49}$$

Due to the fact that s is the product of C and a linear combination of $\sin mK$, one can see that the LC-RK schemes of 1st, 2nd, 5th and 6th order in combination with c.d.-discretisations of the advection operator must be unconditionally unstable: in this case $|A|^2 > 1$ for arbitrary small $C > 0$ (this result follows from the 'small k'-expansion, too, see below).

But also the analysis for c.d.-schemes in combination with LC-RK 3rd, 4th and 7th order is much simpler, because one has to look only for maxima of $|A|^2$ in dependence of one variable s (instead of two), with the simple form '$s = C \times \sum_{l=1}^{m} d_l \sin lK$'. Due to $s(-K) = s(K)$ it is sufficient to inspect the interval $K \in [0, \pi]$. For $K = 0$ and $K = \pi$ there follows $s = 0$ and therefore $|A|^2 = 1$, i.e. no instabilities at the boundaries of this interval. Therefore it is sufficient to search local maxima in $K \in (0, \pi)$ by

$$\frac{d|A|^2}{dK} = \frac{d|A|^2}{ds^2} 2s \frac{ds}{dK} = 0. \tag{50}$$

A graph of $s(K)$ for c.d.-schemes of 2nd, 4th, or 6th order shows, that s possess no zeroes and exactly one extreme value in the open interval $K \in (0, \pi)$ (for $C \neq 0$), which will be determined in the following:

– Centered difference of 2nd order. From (36) follows:

$$s = -C \sin K,$$ (51)

therefore it is sufficient to consider $|A|^2$ at the critical dimensionless wavelength $K_{\text{crit},2} = \pi/2$, which gives

$$s(K = \pi/2) = -C.$$ (52)

– Centered difference of 4th order. From (38) follows that local maxima can occur for

$$\frac{\mathrm{d}s}{\mathrm{d}K} = C\frac{2}{3}\left(\cos^2 K - 2\cos K - \frac{1}{2}\right) = 0.$$

The polynomial $x^2 - 2x - 1/2$ possess the two zeroes $x_{1,2} = 1 \pm \sqrt{3/2}$. Obviously only the solution with the minus sign is possible and it can exist a possible maximum of $|A|^2$ in

$$K_{\text{crit},4} = \arccos\left(1 - \sqrt{\frac{3}{2}}\right) = 1.797\ldots$$ (53)

for which

$$s(K = K_{\text{crit},4}) = -C\left(\frac{1}{2} + \frac{\sqrt{6}}{12}\right)\sqrt{4\sqrt{6} - 6} \approx -1.37222C.$$ (54)

– Centered difference of 6th order. From (40) follows:

$$\frac{\mathrm{d}s}{\mathrm{d}K} = C\frac{12}{30}\left(\cos^3 K - 3\cos^2 K + 3\cos K + \frac{3}{2}\right) = 0.$$

The polynomial $x^3 - 3x^2 + 3x + 3/2$ possess only one real zero $x_1 = 1 - \sqrt[3]{5/2}$ and it follows a possible maximum of $|A|^2$ in

$$K_{\text{crit},6} = \arccos\left(1 - \sqrt[3]{5/2}\right) = 1.936\ldots$$ (55)

This gives

$$s(K = K_{\text{crit},6}) = -C\sqrt{\sqrt[3]{10}\left(\sqrt[3]{22} - \sqrt[3]{5}\right)}\left(\frac{1}{\sqrt{2}} + \frac{\sqrt[6]{2}\sqrt[3]{5}}{6} + \frac{2^{5/6}5^{2/3}}{30}\right) \approx -1.5859C.$$ (56)

The first factor $\mathrm{d}|A|^2/\mathrm{d}s^2$ in (50) also possess zeroes, but Figs. 1–5 of $|A(C,K)|$ show, that the local *maximum* is determined indeed by the zeroes of $\mathrm{d}s/\mathrm{d}K$.

3.1.2. Expansion for long waves

By an expansion of the modulus of the amplification factor $|A(K)|^2$ for small K (i.e. for long waves) necessary conditions for stability can be derived in a relatively simple manner. Instabilities of long waves cannot easily be detected in numerical solutions, because they often grow slowly and do not attract attention like small scale noise. Another undesirable feature of instabilities by long waves is that they cannot be eliminated by filtering. We skip the tedious expansion here but only present the leading terms in Table 1. Table 2 contains the necessary stability criteria derived from them. Especially for the upwind schemes one can get, apart from the familiar $C \geqslant 0$ condition, some non-trivial conditions namely for RK2 and upwind 3rd order, and RK5 and upwind 5th order, and also the instability conclusions for all the RK1 (with the exception of upwind 1st order) and RK2 with upwind 5th order. In [7] a stability constraint $C < 0.30$ was noted for RK2 with upwind 5th order, which is found to be not correct by the analysis presented here. Probably it was found there by numerical experimentation, because this is a very weak instability and hard to see in the amplification factor, Fig. 1.

3.1.3. Discussion of the particular schemes

For some of the schemes analytical expressions can be found for the stability range. For the other cases critical Courant numbers C_{crit} are determined as usual by looking for the smallest C for which the first time a wave number K generates an amplification factor $|A(C,K)| > 1$.
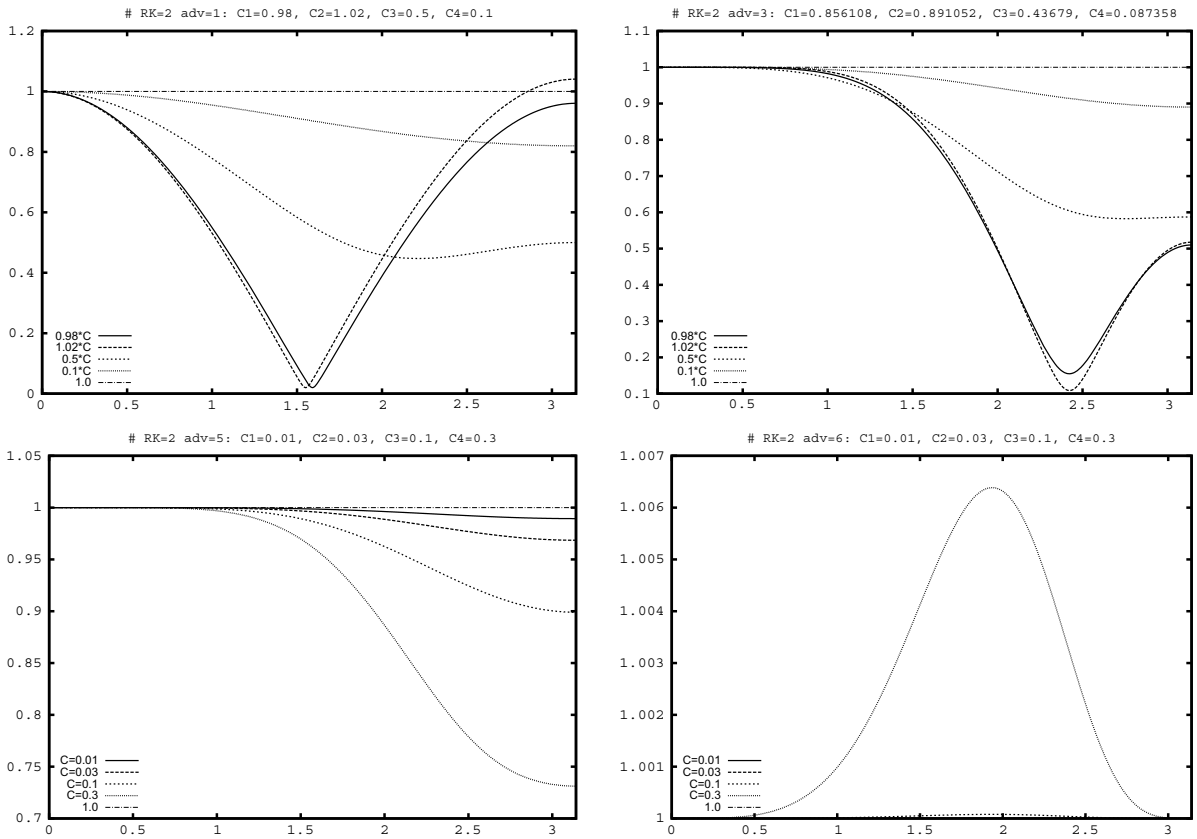
Fig. 1. Amplification factors $|A(C,K)|$ for RK2 and up1, up3, up5, and cd6 (denoted as adv = 1, 3, 5, 6 above each plot) for four different Courant numbers $C = 0.1, 0.5, 0.98, 1.02 \times C_{\text{crit}}$ in the case of $C_{\text{crit}} > 0$ (i.e. up1, up3), $C = 0.01, 0.03, 0.1, 0.3$ in the unstable case (i.e. up5 and cd6). The absolute values of C are written at the top of each plot.

3.1.3.1. LC-Runge–Kutta 1st order (for Euler-forward). For the upwind-scheme, i.e. RK1 with upwind 1st order, it follows from (42) and (35)

$$|A(k)|^2 = 1 + 4\sin^2\frac{K}{2}C(C-1)$$

and therefore the familiar stability constraint $0 < C < 1$.

For all other discretisations, upwind 3rd and 5th order and the centered differences of 2nd, 4th, and 6th order, the long waves are already unstable for all $C \neq 0$. For centered differences of 2nd, 4th, 6th (even order) all waves $K \in (0, \pi)$ are unstable.

3.1.3.2. LC-Runge–Kutta 2nd order. Section 3.1.1 showed that for centered difference of 2nd, 4th and 6th order especially waves with $K = \pi/2$ are unstable and in Section 3.1.2 it was shown that also the long waves are unstable for $C \neq 0$. The lower right panel of Fig. 1 shows also that all waves with $K \in (0, \pi)$ are unstable for cd6; the figures for cd2 and cd4 look like that for cd6 with the maximum lying at $K_{\text{crit},2}$, $K_{\text{crit},4}$, respectively. As remarked above RK2 + upwind 5th order is unstable due to an instability of the long waves. This instability is very weak and hard to see in the lower left panel of Fig. 1.

For RK2 and upwind 1st order, the long waves are stable for $C \geqslant 0$. The amplification factor is

$$|A(k)|^2 = 1 - Ca^2 + \left(\frac{C^2}{2} - \frac{C^3}{2} + \frac{C^4}{4}\right)a^4, \quad a := 2\sin\frac{K}{2}.$$
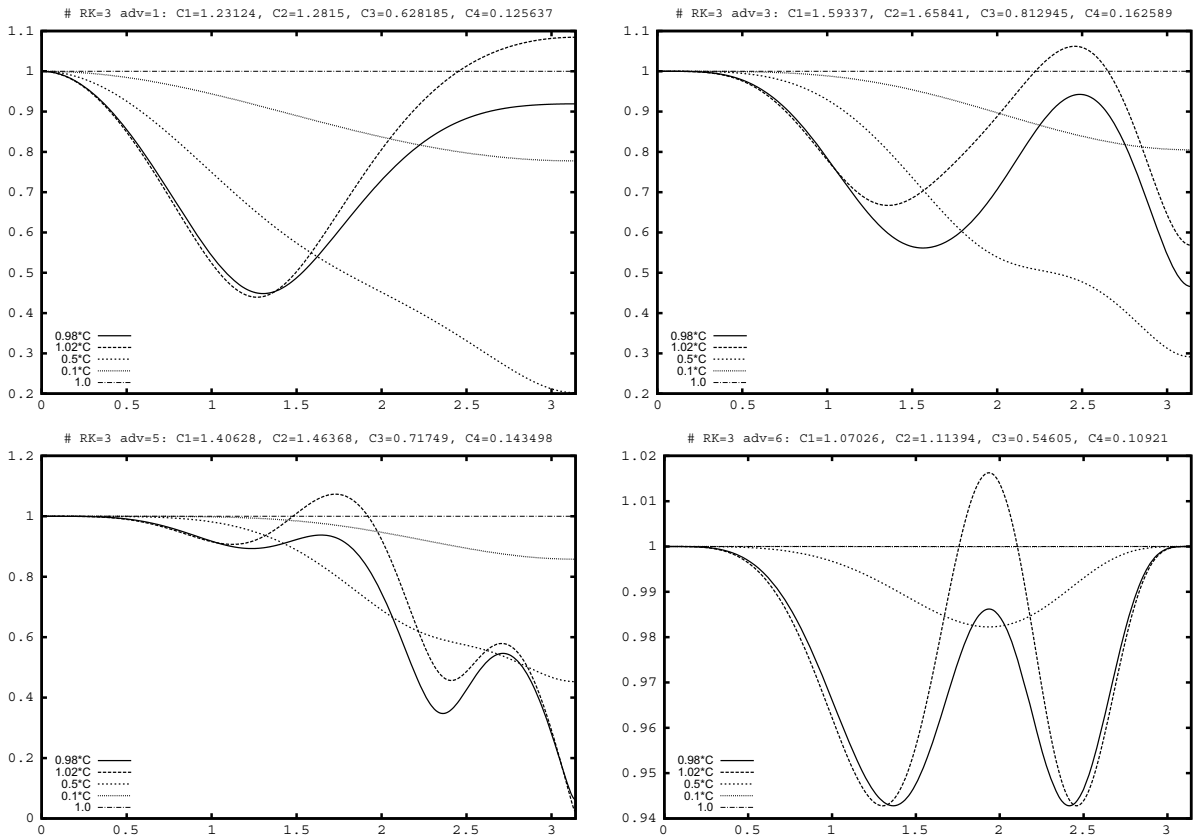
Fig. 2. Amplification factors $|A(C, K)|$ for RK3 and up1, up3, up5, and cd6 (for the choice of C see Fig. 1).

It is plausible (hence not necessary) that short $2\Delta x$-waves, which produce the maximum value of a, become unstable first; this is confirmed graphically by Fig. 1. The amplitude for $2\Delta x$-waves is expressed as

$$A(K = \pi) = 1 - 2C(1 - C) \tag{57}$$

and is therefore stable for $0 < C < 1$.

For RK2 and upwind 3rd order the amplitude sounds for long waves

$$|A(k)|^2 = 1 - K^4\left(\frac{2}{3} - C^3\right)\frac{C}{4} + O(K^6), \tag{58}$$

i.e. long waves are stable for

$$0 \leqslant C \leqslant \left(\frac{2}{3}\right)^{1/3} \approx 0.87358\ldots \tag{59}$$

They become unstable first as can be seen in Fig. 1 and therefore mark the stability range. In this case an analytic expression for C could be found for a result which was known experimentally before [18, p. 106].

3.1.3.3. LC-Runge–Kutta 3rd order. For RK3 and upwind 1st order the long waves remain stable for $C \geqslant 0$ and become unstable for $C < 0$. For $2\Delta x$-waves (which graphically become unstable first) the amplitude is

$$A(K = \pi) = 1 - 2C + 2C^2 - \frac{4}{3}C^3. \tag{60}$$

RK=4 adv=1: C1=1.3648, C2=1.4205, C3=0.696325, C4=0.139265

RK=4 adv=3: C1=1.71035, C2=1.78017, C3=0.87263, C4=0.174526
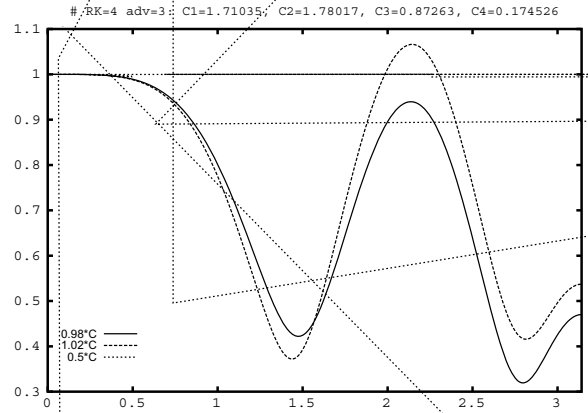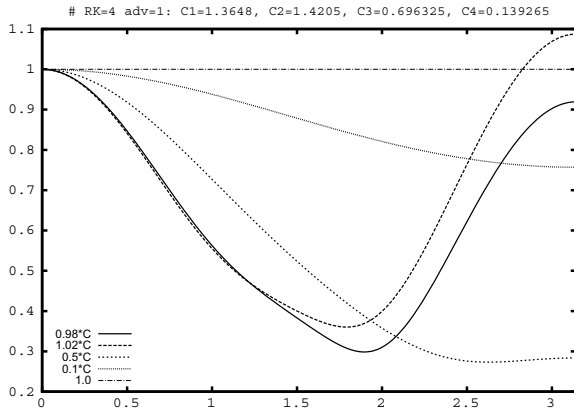
Therefore we are looking for real C, for which the modulus of this amplitude equals 1. Because all coefficients are real, either $A = +1$ (which leads to $C = 0$, the other solutions are not real) or $A = -1$ which leads to the only real solution

$$C_{3,1,\text{crit}} = \frac{1}{2}\left(a - \frac{1}{a} + 1\right), \quad a = (4 + \sqrt{17})^{1/3} \tag{61}$$

and therefore stability for $0 \leqslant C < C_{3,1,\text{crit}} = 1.25637\ldots$.

For RK3 and centered difference of 2nd order, the long waves are stable for all C. From the behaviour of the $4\Delta x$-waves, $|A(K = \pi/2)|^2 = 1$, follows the critical Courant number $C_{\text{crit}} = \sqrt{3} = 1.73205\ldots$.

For RK3 and upwind 3rd order the long waves remain stable for $C \geqslant 0$; short waves with approximately $K \approx 2.473$ become unstable for $C > 1.62589\ldots$.

For RK3 and centered differences 4th order the long waves are stable for all C. Short waves become unstable at $K_{\text{crit},4} = \arccos\left(1 - \sqrt{3/2}\right) = 1.797\ldots$; from $|A(K = K_{\text{crit},4})|^2 = 1$ follows the critical wave number

$$C_{3,4,\text{crit}} := \sqrt{\frac{3}{\frac{2}{3}\sqrt{6} + \frac{1}{4}}} = 1.26222\ldots \tag{62}$$

For RK3 and upwind 5th order long waves remain stable for all C; short waves with approximately $K \approx 1.693\ldots$ become unstable for $C > 1.43498\ldots$.

For RK3 and centered differences 6th order long waves remain stable for all C; short waves with $K_{crit,6} = \arccos(1 - \sqrt[3]{5/2}) = 1.936\ldots$ become unstable (from $|A(K = K_{\text{crit},6})|^2 = 1$) at

Table 1
Expansion of the amplification factor $|A(k)|^2$ for small K

	up1	cd2
LC-RK1	$1 + K^2 \cdot C(C-1) + O(K^4)$	$1 + K^2 \cdot C^2 + O(K^4)$
LC-RK2	$1 - K^2 C + O(K^4)$	$1 + K^4 C^4/4 + O(K^6)$
LC-RK3	$1 - K^2 C + O(K^4)$	$1 - K^4 C^4/12 + O(K^6)$
LC-RK4	$1 - K^2 C + O(K^4)$	$1 - K^6 C^6/72 + O(K^8)$
LC-RK5	$1 - K^2 C + O(K^4)$	$1 + K^6 C^6/360 + O(K^8)$
LC-RK6	$1 - K^2 C + O(K^4)$	$1 + K^8 C^8/2880 + O(K^{10})$
LC-RK7	$1 - K^2 C + O(K^4)$	$1 - K^8 C^8/20160 + O(K^{10})$
	up3	**cd4**
LC-RK1	$1 + K^2 \cdot C^2 + O(K^4)$	$1 + K^2 \cdot C^2 + O(K^6)$
LC-RK2	$1 - K^4 (2/3 - C^3)C/4 + O(K^6)$	$1 + K^4 C^4/4 + O(K^8)$
LC-RK3	$1 - K^4 C(C^3 + 2)/12 + O(K^6)$	$1 - K^4 C^4/12 + O(K^6)$
LC-RK4	$1 - K^4 C/6 + O(K^6)$	$1 - K^6 C^6/72 + O(K^8)$
LC-RK5	$1 - K^4 C/6 + O(K^6)$	$1 + K^6 C^6/360 + O(K^8)$
LC-RK6	$1 - K^4 C/6 + O(K^6)$	$1 + K^8 C^8/2880 + O(K^{10})$
LC-RK7	$1 - K^4 C/6 + O(K^6)$	$1 - K^8 C^8/20160 + O(K^{10})$
	up5	**cd6**
LC-RK1	$1 + K^2 C^2 + O(K^6)$	$1 + K^2 C^2 + O(K^8)$
LC-RK2	$1 + K^4 C^4/4 + O(K^6)$	$1 + K^4 C^4/4 + O(K^{10})$
LC-RK3	$1 - K^4 C^4/12 + O(K^6)$	$1 - K^4 C^4/12 + O(K^6)$
LC-RK4	$1 - K^6 C(12/5 + C^5)/72 + O(K^8)$	$1 - K^6 C^6/72 + O(K^8)$
LC-RK5	$1 + K^6 C(C^5 - 12)/360 + O(K^8)$	$1 + K^6 C^6/360 + O(K^8)$
LC-RK6	$1 - K^6 C/30 + O(K^8)$	$1 + K^8 C^8/2880 + O(K^{10})$
LC-RK7	$1 - K^6 C/30 + O(K^8)$	$1 - K^8 C^8/20160 + O(K^{10})$

Table 2
Necessary stability conditions, which are *only* determined by long waves ($K \to 0$)

	up1	cd2	up3	cd4	up5	cd6
LC-RK1	$0 \leqslant C \leqslant 1$	Unstable	Unstable	Unstable	Unstable	Unstable
LC-RK2	$C \geqslant 0$	Unstable	$0 \leqslant C \leqslant \sqrt[3]{2/3}$	Unstable	Unstable	Unstable
LC-RK3	$C \geqslant 0$	–	$C \geqslant 0$	–	–	–
LC-RK4	$C \geqslant 0$	–	$C \geqslant 0$	–	–	–
LC-RK5	$C \geqslant 0$	Unstable	$C \geqslant 0$	Unstable	$0 \leqslant C \leqslant \sqrt[5]{12}$	Unstable
LC-RK6	$C \geqslant 0$	Unstable	$C \geqslant 0$	Unstable	$C \geqslant 0$	Unstable
LC-RK7	$C \geqslant 0$	–	$C \geqslant 0$	–	$C \geqslant 0$	–

$$A(K = \pi) = 1 - 2C + 2C^2 - \frac{4}{3}C^3 + \frac{2}{3}C^4. \tag{64}$$

Real solutions for $A(K = \pi) = +1$ exist for $C = 0$ and

$$C_{4,1,\text{crit}} = a/6 - 10/(3a) + 2/3, \quad a = (172 + 36\sqrt{29})^{1/3} \tag{65}$$

and therefore holds the stability range $0 \leqslant C < C_{4,1,\text{crit}} = 1.392646782\ldots$.

For RK4 and centered difference 2nd order the amplification factor sounds

$$|A(k)|^2 = 1 - \frac{1}{72}(C \sin K)^6 \left(1 - \frac{C^2 \sin^2 K}{8}\right).$$

As for all cd2 schemes $4\Delta x$-waves become unstable first which leads to $C < \sqrt{8} = 2.828427\ldots$

For the schemes with spatial order higher than 2 no analytical solutions could be found so far; we refer to Tables 3 and 5 for the values found by a numerical search of the maximum of $|A(C,K)|$.

3.1.3.5. LC-Runge–Kutta 5th and 6th order. As mentioned above (Sections 3.1.1 and 3.1.2) all the centered difference schemes of 2nd, 4th, and 6th order are unconditionally unstable. The amplification factors $|A(C,K)|$

Table 3
Limits for stable Courant numbers C_{crit}

	up1	cd2	up3	cd4	up5	cd6
LC-RK1	1	0	0	0	0	0
LC-RK2	1	0	0.87358	0	0	0
LC-RK3	1.25637	1.73205	1.62589	1.26222	1.43498	1.09210
LC-RK4	1.39265	2.82843	1.74526	2.06120	1.73197	1.78339
LC-RK5	1.60852	0	1.95350	0	1.64375	0
LC-RK6	1.77672	0	2.31039	0	1.86707	0
LC-RK7	1.97706	1.76442	2.58599	1.28581	2.26079	1.11251

Table 4
Analoguous to Table 3: limits for stable Courant numbers, *only* analytical results, as far as known

	up1	cd2	up3	cd4	up5	cd6
LC-RK1	1	0	0	0	0	0
LC-RK2	1	0	$\sqrt[3]{2/3}$	0	0	0
LC-RK3	$C_{3,1,\mathrm{crit}}$	$\sqrt{3}$		$C_{3,4,\mathrm{crit}}$		$C_{3,6,\mathrm{crit}}$
LC-RK4	$C_{4,1,\mathrm{crit}}$	$\sqrt{8}$				
LC-RK5		0		0	$\sqrt[5]{12}$	0
LC-RK6		0		0		0
LC-RK7						

For the critical Courant numbers $C_{3,1,\mathrm{crit}}, \ldots$, see Eqs. (61), (62), (63), and (65).

Table 5
Dimensionless wave number $K = k\Delta x$, which becomes unstable first

	up1	cd2	up3	cd4	up5	cd6
LC-RK1	All	All	$\rightarrow 0$	All	$\rightarrow 0$	All
LC-RK2	π	All	$\rightarrow 0$	All	$\rightarrow 0$	All
LC-RK3	π	$\pi/2$	2.473	1.797	1.693	1.936
LC-RK4	π	$\pi/2$	2.141	1.797	2.298	1.936
LC-RK5	π	All	1.843	All	$\rightarrow 0$	All
LC-RK6	π	All	1.685	All	1.686	All
LC-RK7	π	$\pi/2$	2.213	1.797	1.669	1.936

'All' means: all wavelengths with $0 < K < \pi$, '$\rightarrow 0$' means: long waves become unstable.

look qualitatively rather similar to those for RK2 + cd6, but with different values for the maximum and of course with the maximum of $|A(C, K)|$ at the critical wavelengths $K_{\mathrm{crit},2}$, $K_{\mathrm{crit},4}$, and $K_{\mathrm{crit},6}$, respectively. The $|A(C, K)|$ for up1 look rather similar to that of RK4 + up1. For the upwind schemes no analytical solutions could be found. The long waves only require $C \geqslant 0$ (see Table 1). Again we refer to Tables 3 and 5 for the numerical determination of the stability range. One exception is RK5 + upwind 5th order for which an analytical solution could be found.

For RK5 and upwind 1st order the amplitude sounds for $2\Delta x$-waves

$$A(K = \pi) = 1 - 2C + 2C^2 - \frac{4}{3}C^3 + \frac{2}{3}C^4 - \frac{4}{15}C^5. \tag{66}$$

Because the latter is a polynomial of the 5th degree, a closed form expression for the roots of $A(K = \pi) = -1$ (which solely determines the stability range) is not available. The numerically found constraint is $C < 1.60852\ldots$.

For RK5 and upwind 5th order the first short wave which becomes unstable is $K_{\mathrm{crit}} = 2.0402\ldots$ which requires $C < 1.734914\ldots$. But the long waves, for which

$$|A(k)|^2 = 1 + K^6 \frac{C}{360}\left(C^5 - 12\right) + \mathrm{O}(K^8)$$

holds, produce the stronger constraint $0 \leqslant C < \sqrt[5]{12} = 1.64375\ldots$.

For RK6 and upwind 1st order the amplitude is for $2\Delta x$-waves

$$A(K = \pi) = 1 - 2C + 2C^2 - \frac{4}{3}C^3 + \frac{2}{3}C^4 - \frac{4}{15}C^5 + \frac{4}{45}C^6. \tag{67}$$

Again no closed form expression is available for the roots of $A(K = \pi) = +1$ (which solely determines the stability range) thus they need to be found numerically which delivers the constraint $C < 1.77672\ldots$.

3.1.3.6. LC-Runge–Kutta 7th order. It seems also not possible to find analytical solutions for critical Courant numbers. The long waves generate only $C \geqslant 0$ as a necessary stability constraint (see Table 1). The stability limits where obtained numerically as described above and we refer again to Table 3 and 5. Fig. 5 shows the amplification factors for up3, up5, and cd6. The figures for cd2 and cd4 look like that for cd6 with the maximum shifted to $K_{\text{crit},2}$, and $K_{\text{crit},4}$, respectively; those for up1 looks rather similar to that for RK4 + up1.

4. Numerical experiments

In this section some numerical experiments are carried out to highlight the practical meaning of the stability limits found in the previous section. For this purpose a 1D-cone function

$$q(x, t = 0) = \begin{cases} 1 + x/b, & -b \leqslant x \leqslant 0, \\ 1 - x/b, & 0 \leqslant x \leqslant b, \\ 0, & \text{otherwise} \end{cases}$$

is used for the initial values. Its Fouriertransform is $\tilde{q}(k) = 2b(1 - \cos(kb))/(kb)^2$, which has a main maximum at $k = 0$ and several rapidly decaying side maxima at $kb = 3\pi, 5\pi, 7\pi, \ldots$. We choose a width of $b = 8.5\Delta x$ which means on the one hand that the cone is rather good resolved, but on the other hand that both fastest growing (dimensionless) wavenumbers $K_{\text{crit},4}$ and $K_{\text{crit},6}$ are lying near the 2nd side maximum of $\tilde{q}(k)$. The grid consists of 1000 gridpoints with constant $\Delta x = 1$, the boundary conditions are periodic.

In Table 6 the approximate number of timesteps for two different Courant numbers is plotted, for which the schemes doubtlessly become unstable. 'Doubtless' means, that the noise amplitude becomes bigger than the initial amplitude of the 1D-cone function. In all the other cases where the schemes are claimed to be stable up to a Courant number C_{crit} (see Table 3) this numerical experiment actually results in no instability for at least $10^8/C$ timesteps, if the advection equation was solved with a Courant number $C = 0.99 \cdot C_{\text{crit}}$. Such a large number of timesteps would be used only in highly resolved ($\Delta x \sim 10$ km) global climate simulations for several hundred of years.

A numerical example of a slow instability is shown in Fig. 6. Even after a half million timesteps RK5 + cd4 shows almost no numerical noise apart from a strong dispersion of an otherwise relatively good captured peak. The blow up takes place after more than two million timesteps.

Table 7 shows the leading terms in C of the amplification factor $|A(k, C)|^2$ for the fastest growing wavenumber K_{crit} for centered difference schemes. These are calculated by inserting s from Eqs. (52), (54), (56), respectively, into the amplification factors (43)–(49). The results of Table 6 match very well to these expansions. For

Table 6
Approximate number of timesteps for two different Courant numbers, for which the schemes become doubtlessly unstable

	$C = 0.5$	$C = 0.25$
LC-RK2 + up5	4200	3.2×10^6
LC-RK2 + cd4	200	3600
LC-RK2 + cd6	120	2000
LC-RK5 + cd4	50,000	2.8×10^6
LC-RK5 + cd6	25,000	1.2×10^6
LC-RK6 + cd4	800,000	
LC-RK6 + cd6	240,000	
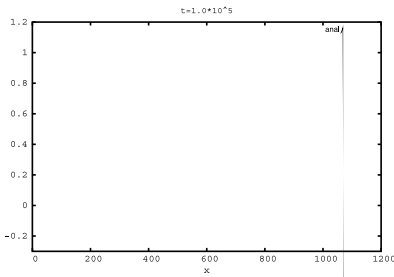
LC-RK5, for example, the cd4 discretization takes about two times more timesteps to become unstable than cd6. Halving of C increases the number of timesteps until a blow up to a factor of about 16 for LC-RK2 and a factor of about 64 for LC-RK5 and would be taken about a factor of 256 for LC-RK6. Therefore no values are given for LC-RK6 and $C = 0.5$; this scheme is nearly stable for any practical purposes at least up to this Courant number. The relatively small deviations from 1 explain, why the instabilities take such a long time to grow exponentially.

It should be mentioned here, that the unconditional instability of RK5 and RK6 is a property of the LC-RK-schemes. One can in fact try to improve the stability by searching for schemes which have a reduced order compared to their stage also in the linear case. This approach is used in [10,11]. [10] found RK-schemes with $C = 1.53$ for a 5-stage RK and $C = 1.655$ for a 6-stage RK with a cd2 spatial discretization, whereas their 4-stage RK is even unconditionally unstable. Better stability properties were found by [11], whose 5-stage ('RKo5s') and 6-stage RK-scheme ('RKo6s') allow $C = 3.558$ and $C = 3.942$ with cd2, respectively.

The instabilities occurring in the schemes of Table 7 arise due to small wavelengths and can be cured in principle by applying additional smoothing. Due to the smallness of the unstable amplification factor a relatively small value for the damping coefficient should be sufficient to stabilize the schemes for small Courant numbers. The $|A|^2$ in Table 7 give an estimation for the strength of such a smoothing filter. But nevertheless the lack of a clear stability limit constrains the usage of these schemes.

The fact that some of the schemes of Table 6 hide their instabilities for a long time until the solution blows up rises the question if this is due to an inadequate form of the stability measure. Indeed, the Lax equivalance theorem states the convergence of a linear scheme if the scheme is consistent and Lax–Richtmyer-stable [21]. Lax–Richtmyer-stability is a weaker constraint than the strong stability used here since it requires only that a norm of the amplification matrix after the needed number of timesteps is bounded by an arbitrary function of the total time T alone: $\|A^n\| < C(T)$. This is the case, if $\|A\| < 1 + \alpha\,\Delta t$, with a constant α independent from Δx, Δt. As can be seen from Table 7 this is fulfilled if Δt tends to zero faster than Δx. Normally this is an undesirable behaviour for an advection scheme. But in any practical application not only convergence of a solution is needed but also the lack of noise, which increases in time and destroys the true solution. [22] mentions that for non-growing solutions (as for the linear advection equation) the strong stability constraint $\|A^n\| \leqslant 1$ should be used, for which a sufficient condition is $\|A\| \leqslant 1$. The relation between the norm of a matrix and its spectral radius, i.e. the maximum eigenvalue is often very complicated. But as it is stated in [22] inspection of the eigenvalues detects at least the exponential growing of modes, whereas linear growing modes could occur even if all eigenvalues are less than one. Therefore the von-Neumann stability analysis used here should give a satisfactory measure for stability of the advection equation.
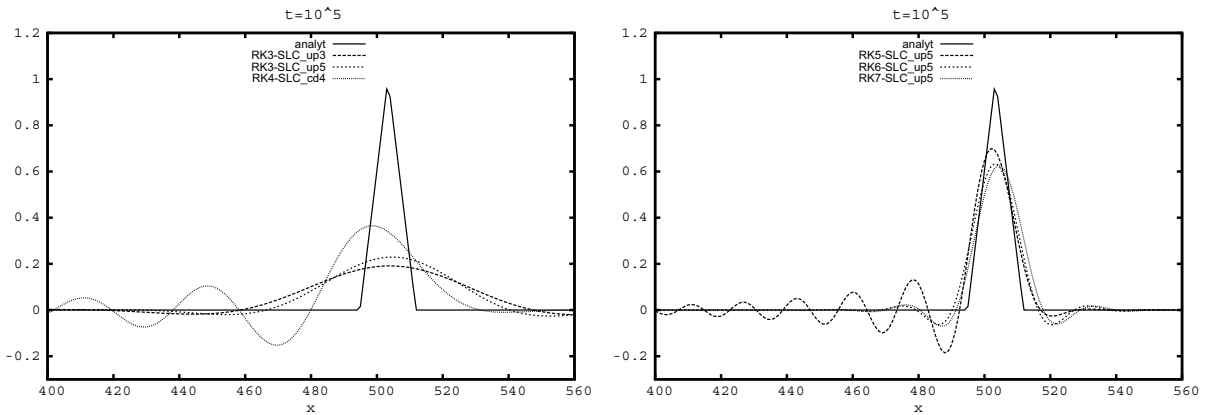
Fig. 7. 'Long time' numerical solution of the advection equation with RK3 + up3, RK3 + up5, RK4 + cd4 (left panel) and RK5 + up5, RK6 + up5, RK7 + up5 (right panel), analytic solution: solid line. Each scheme used with the greatest possible Courant number C_{crit}. Simulation time $t = 10^5$, i.e. after $10^5/C_{crit}$ timesteps.

To get an impression about the accuracy of the stable schemes at the stability limit, Fig. 7 shows the numerical solution of the advection equation where each scheme was used with its highest possible Courant number C_{crit}. Results are shown after $t = 10^5$ which is equivalent to a number of $10^5/C_{crit}$ timesteps. The left panel shows the relatively efficient schemes (see Section 6 about efficiency). RK3 + up3 and RK3 + up5 show a strong diffusion error, whereas the next efficient RK4 + cd4 has less diffusion error but a stronger dispersion error. The other stable RK3 and RK4 schemes behave rather similar but have less efficiency than these three schemes. The right panel shows schemes with much less efficiency but obviously bigger accuracy: RK5, RK6 and RK7 with up5. Figs. 4 and 5 already give a hint for this better behaviour, because the range with $|A| \approx 1$ goes to higher wavenumbers compared to the other discretizations. RK5, RK6, RK7 with the other spatial discretizations have no advantage in accuracy and compare more to the schemes on the left panel.

5. Multi-dimensional advection

Multi-dimensional advection of course can be done by using an appropriate multi-dimensional scheme. [23] presented an example for stabilizing a multi-dimensional Crowley-scheme. But this more straightforward way is not employed in operational models because it generally requires more operations than the splitting of the multi-dimensional operator into several 1D advection schemes (besides the Crowley method delivers a higher order discretization in space and time and is therefore not well suited for combination with a Runge–Kutta method which requires Euler forward steps). As an example we look to the two-dimensional advection equation

$$\frac{\partial \phi}{\partial t} = -c_x \frac{\partial \phi}{\partial x} - c_y \frac{\partial \phi}{\partial y}. \tag{68}$$

If we discretize both spatial derivatives with the same scheme (one of the proposed above) and add the appropriate tendencies in every Runge–Kutta-substep, it follows for the semi-discretized amplitude $(Cd)_{tot}$ (analogously defined as in Eq. (34))

$$(Cd)_{tot} = C_x d_{1D}(K_x) + C_y d_{1D}(K_y) \tag{69}$$

with $C_i = c_i \Delta t / \Delta x_i$ and $K_i = k_i \Delta x_i$. d_{1D} are the appropriate factors derived in Section 3. We remark that with the exception of the upwind 1st order scheme all spatial discretisations are unstable with an Euler-forward step (Table 3). Therefore the often applied operator splitting of the directions called locally one-dimensional (LOD)-methods [18] is not possible (LOD-methods can guarantee stability by producing the cross derivative terms and maintain positive definiteness, if the 1D-operators have this property). At least one advantage of

adding tendencies is that the sequence of operations does not play a role. If we consider in particular waves with $K_x = K_y = K$ we get

$$(Cd)_{\text{tot}} = (C_x + C_y) \; d_{1D}(K). \tag{70}$$

Therefore for this special wave vector we can transform the stability problem to the purely 1D-case considered in the section before and we get a *necessary* stability constraint

$$|C_x| + |C_y| < C_{\text{crit}} \tag{71}$$

with C_{crit} from Table 3 (of course, the modulus of each C_i is valid only, if the upwind schemes are properly implemented and can handle both velocity directions). So for example for Runge–Kutta 2nd order with upwind 3rd order

$$|C_x| + |C_y| < \sqrt[3]{2/3}. \tag{72}$$

Analogously we find for advection in n dimensions as a necessary stability constraint

$$|C_1| + \cdots + |C_n| < C_{\text{crit}}. \tag{73}$$

Although this is only a necessary condition, one can find by numerical experimentation that it is often also a sufficient condition. This is in good agreement with the result cited in [23], that diagonal waves, i.e. waves with $K_x = K_y$, are the most unstable ones.

6. Conclusions

In this paper, the stability properties of Runge–Kutta methods in combination with optimal-order finite difference spatial discretisations of the linear advection equation were inspected. The emphasis lies on the classical 'order = stage' RK-schemes, which have the high approximation order also for nonlinear equations. It was shown that the stability statements can be extended to the much wider class of LC-RK methods. In some cases even analytical expressions for the critical Courant number could be found in Section 3, collected in Table 4. Perhaps that is more satisfying for the theoretically oriented reader. Of course, the practical critical wave number (and consequently the critical Courant number) slightly depends from the grid point distribution and therefore from the actually available wave numbers.

The stability statements of Section 2 can be extended to a relatively broad range of linear ODE's and in particular to many linear, semi-discretized PDE's and PDE-systems, as long as the discretisation keeps linear, too. An example could be an advection–diffusion equation

$$\frac{\partial q}{\partial t} = c(\mathbf{r}) \nabla q + \nabla K(\mathbf{r}) \nabla q, \tag{74}$$

where the coefficients do not need to be constant as long as they are time independent. One could have in mind velocity and diffusion coefficient fields which have to be transformed in a terrain following coordinate system. Another example would be a linearised Korteveg-deVries equation, linearised shallow equations or other coupled systems of such PDE's. In the case that an analytical stability analysis is impossible, it could be sufficient to inspect linear stability ranges by numerical experimentation. In this case one can use the simple LC-RK method of order N defined by Eq. (22). Of course, one should consider if the discretisation of the generally nonlinear system is better done with an 'order = stage' Runge–Kutta-scheme of Nth order.

For an assessment of the methods inspected here, there are to consider also other characteristics apart from (linear and non-linear) stability as accuracy, conservation properties, further consistency conditions and naturally also efficiency. Addressing to accuracy, one should obey that the temporal order is reduced e.g. by subcycling to at most 2nd order. For the spatial approximation order one surely would like to go away from the traditional centered differences 2nd order to schemes of higher order to better represent small scale features of the fields. Whereas shock capturing does not play an essential role in the most meteorological applications, the approximation error on the other hand can be strongly enhanced in the case of not smooth enough fields. In meteorological applications (in particular weather forecast) one will prefer spatial discretisations in the range of 3rd–5th order, probably not higher than 6th order.

As a (rough) measure of efficiency, [5] define an 'effective Courant number' $C_{\text{eff}} = C/N$ for an N-stage scheme. However, in the case of subcycling it must be pointed out that the longer is a RK substep, the more

Table 8
The 'effective Courant number' $C_{\mathrm{eff}} := C_{\mathrm{crit}}/N$ as defined in [5]

	up1	cd2	up3	cd4	up5	cd6
LC-RK1	1	0	0	0	0	0
LC-RK2	0.5	0	0.437	0	0	0
LC-RK3	0.419	0.577	0.542	0.421	0.478	0.364
LC-RK4	0.348	0.707	0.436	0.515	0.433	0.446
LC-RK5	0.322	0	0.391	0	0.329	0
LC-RK6	0.296	0	0.385	0	0.311	0
LC-RK7	0.282	0.252	0.369	0.184	0.323	0.159

substeps of the fast processes with a short timestep have to be carried out. Therefore the different substeps contribute in a different manner to efficiency. Moreover the different spatial discretizations need more computation time by increasing the stencil. Apart from these limitations of the measure C_{eff}, we can see in Table 8 that the 'efficient Courant number' is relatively large for the combinations 'LC-RK3 + up3' and 'LC-RK3 + up5'. The latter is used indeed in the WRF model and also in the very short range forecast model COSMO-DE of the DWD, the former is planned to be used in the regional model COSMO-EU. The efficiency of 'LC-RK3 + up5' would be even surpassed by 'LC-RK4 + cd4', which tends to be more dispersive. If one can tolerate a small spatial discretization order then 'LC-RK4 + cd2' is obviously the most efficient choice. Usage of LC-RK methods with order $N > 4$ for pure advection seems neither to be justified by the temporal order nor by efficiency. If one is interested to use even higher order RK-methods, then one has to look for schemes whose order is less than the stage also for linear differential equations.

Appendix A. Coefficients of the (LC)-Runge–Kutta methods of order N

In this section the general conditions for 'order = stage' RK methods ([13]; the conditions up to 5th order are also explicitly given in [14], Eqs. (7) and (25)) and their subset for the LC-RK methods up to 4th order are presented.

The 1st order Runge–Kutta (or Euler method or simply the Euler forward step) has only the consistency condition

$$\beta_{21} = 1 \tag{A.1}$$

as a constraint; of course the same as for LC-RK 1st order.

The 2nd order Runge–Kutta (and LC-RK) has the truncation error $O(\Delta t^3)$ if the 2 conditions

$$\beta_{31} + \beta_{32} = 1, \tag{A.2}$$

$$\beta_{32}\beta_{21} = \frac{1}{2} \tag{A.3}$$

are fulfilled. Examples are the modified Euler method [6] or the Heun method (see also [22]).

The 3rd order RK scheme has four conditions for six coefficients β_{ij}

$$\beta_{41} + \beta_{42} + \beta_{43} = 1, \tag{A.4}$$

$$\beta_{42}\beta_{21} + \beta_{43}(\beta_{31} + \beta_{32}) = 1/2, \tag{A.5}$$

$$\beta_{42}\beta_{21}^2 + \beta_{43}(\beta_{31} + \beta_{32})^2 = 1/3, \tag{A.6}$$

$$\beta_{43}\beta_{32}\beta_{21} = 1/6 \tag{A.7}$$

(see [13, p. 173]). Two standard schemes are shown in the following Butcher-tableaus:

$$
\begin{array}{c|ccc}
0 & & & \\
\frac{1}{3} & \frac{1}{3} & & \\
\frac{2}{3} & 0 & \frac{2}{3} & \\
\hline
 & \frac{1}{4} & 0 & \frac{3}{4}
\end{array}
\qquad
\begin{array}{c|ccc}
0 & & & \\
1 & 1 & & \\
\frac{1}{2} & \frac{1}{4} & \frac{1}{4} & \\
\hline
 & \frac{1}{6} & \frac{1}{6} & \frac{2}{3}
\end{array}
$$

where the 3rd order RK methods cited as RK3a (left) and RK3b (right) in [19] are shown. The right one is also denoted as TVD-RK3 in [20]. [15] proposed a memory saving RK3 variant. (A.4), (A.5), and (A.7) are the general conditions for a 3rd order LC-RK method.

The 4th order Runge–Kutta method has 8 conditions for 10 coefficients β_{ij}:

$$\beta_{51} + \beta_{52} + \beta_{53} + \beta_{54} = 1, \tag{A.8}$$

$$\beta_{52}\beta_{21} + \beta_{53}\alpha_3 + \beta_{54}\alpha_4 = \frac{1}{2}, \tag{A.9}$$

$$\beta_{52}\beta_{21}^2 + \beta_{53}\alpha_3^2 + \beta_{54}\alpha_4^2 = \frac{1}{3}, \tag{A.10}$$

$$\beta_{54}(\beta_{42}\beta_{21} + \beta_{43}\alpha_3) + \beta_{53}\beta_{32}\beta_{21} = \frac{1}{6}, \tag{A.11}$$

$$\beta_{52}\beta_{21}^3 + \beta_{53}\alpha_3^3 + \beta_{54}\alpha_4^3 = \frac{1}{4}, \tag{A.12}$$

$$\beta_{54}(\beta_{42}\beta_{21}^2 + \beta_{43}\alpha_3^2) + \beta_{53}\beta_{32}\beta_{21}^2 = \frac{1}{12}, \tag{A.13}$$

$$\beta_{54}\alpha_4(\beta_{42}\beta_{21} + \beta_{43}\alpha_3) + \beta_{53}\beta_{32}\beta_{21}\alpha_3 = \frac{1}{8}, \tag{A.14}$$

$$\beta_{54}\beta_{43}\beta_{32}\beta_{21} = \frac{1}{24}, \tag{A.15}$$

with the abbreviations $\alpha_3 = \beta_{31} + \beta_{32}$ and $\alpha_4 = \beta_{41} + \beta_{42} + \beta_{43}$ following Eq. (9). One example is the so called 'classical Runge–Kutta' method which can be found in nearly every textbook about ODE solvers [22]. Four of these conditions, namely (A.8), (A.9), (A.11) and (A.15) are the general conditions for a 4th order LC-RK method.

References

[1] T. Davies, M.J.P. Cullen, A.J. Malcolm, M.H. Mawson, A. Staniforth, A.A. White, N. Wood, A new dynamical core for the Met Office's global and regional modelling of the atmosphere, Quart. J. Roy. Meteor. Soc. 131 (608) (2005) 1759–1782.

[2] J.B. Klemp, R.B. Wilhelmson, The simulation of three-dimensional convective storm dynamics, J. Atmos. Sci. 35 (1978) 1070–1096.

[3] E.J. Kubatko, J.J. Westerink, C. Dawson, Semi discrete discontinuous Galerkin methods and stage-exceeding-order, strong-stability-preserving Runge–Kutta time discretizations, J. Comput. Phys. 222 (2007) 832–848.

[4] C.-W. Shu, Total-variation diminishing time discretizations, SIAM J. Sci. Stat. Comput. 9 (6) (1988) 1073–1084.

[5] S.J. Ruuth, R.J. Spiteri, High-order strong-stability-preserving Runge–Kutta methods with downwind-biased spatial Discretizations, SIAM J. Numer. Anal. 42 (3) (2004) 974–996.

[6] L.J. Wicker, W.C. Skamarock, A time-splitting scheme for the elastic equations incorporating second-order Runge–Kutta time differencing, Mon. Weather Rev. 126 (1998) 1992–1999.

[7] L.J. Wicker, W.C. Skamarock, Time splitting methods for elastic models using forward time schemes, Mon. Weather Rev. 130 (2002) 2088–2097.

[8] A. Bott, A positive definite advection scheme obtained by nonlinear renormalization of the advective fluxes, Mon. Weather Rev. 117 (5) (1989) 1006–1015.

[9] A. Staniforth, J. Côté, Semi-lagrangian integration schemes for atmospheric models – a review, Mon. Weather Rev. 119 (1991) 2206–2223.

[10] F.Q. Hu, M.Y. Hussaini, J. Manthey, Low-dissipation and -dispersion Runge–Kutta schemes for computational acoustics, ICASE Report, NASA-Langley, 1994, pp. 94–102.

[11] C. Bogey, C. Bailly, A family of low dispersive and low dissipative explicit schemes for flow and noise computations, J. Comput. Phys. 194 (2004) 194–214.

[12] Z. Haras, S. Tasan, Finite difference schemes for long-time integration, J. Comput. Phys. 114 (1994) 265–279.

[13] J.C. Butcher, The Numerical Analysis of Ordinary Differential Equations, Wiley, 1987.

[14] P. Albrecht, The Runge–Kutta theory in a nutshell, SIAM J. Numer. Anal. 33 (5) (1996) 1712–1735.

[15] J. Williamson, Low-storage Runge–Kutta schemes, J. Comput. Phys. 35 (1980) 48–56.

[16] J.D. Lambert, Numerical Methods for Ordinary Differential Systems, J. Wiley and Sons, Chichester, 1991.

[17] E. Hairer, G. Wanner, Solving Ordinary Differential Equations II: Stiff and Differential-Algebraic Problems, second revised ed., Springer, Berlin, 2002.

[18] W. Hundsdorfer, J. Verwer, Numerical Solution of Time-Dependent Advection–Diffusion–Reaction Equations, Springer, Berlin, 2003.
[19] W. Hundsdorfer, B. Koren, M. van Loon, J.G. Verwer, A positive finite-difference advection scheme, J. Comput. Phys. 117 (1995) 35–46.
[20] X.-D. Liu, S. Osher, T. Chan, Weighted essentially non-oscillatory schemes, J. Comput. Phys. 115 (1994) 200–212.
[21] R.J. LeVeque, Finite Difference Methods for Ordinary and Partial Differential Equations, Society for Industrial and Applied Mathematics (SIAM), Philadelphia, 2007.
[22] D.R. Durran, Numerical Methods for Wave Equations in Geophysical Fluid Dynamics, Springer, New York, 1998.
[23] P.K. Smolarkiewicz, The multi-dimensional Crowley advection scheme, Mon. Weather Rev. 110 (1982) 1968–1983.